

THE RADIO BRIGHTNESS DISTRIBUTIONS OVER FOUR DISCRETE SOURCES OF COSMIC NOISE

By B. Y. MILLS*

[*Manuscript received August 3, 1953*]

Summary

Brightness distributions have been obtained across the four radio sources, Cygnus-A, Taurus-A, Virgo-A, and Centaurus-A, using a two-aerial interferometer of a special type in which the aerial spacing and the azimuth angle of the axis may be varied over a wide range. Radio isophotes have been constructed for three of the sources from these results, making some simple assumptions as to their form. The isophotes bear some relation to optical features of the nebulae with which the sources have been identified and their radio and optical sizes are similar. The remaining source, Cygnus-A, is unfavourably situated for observations from Sydney, and the results are less complete.

I. INTRODUCTION

The nature of the discrete radio sources has been the subject of speculation since their discovery by Bolton and Stanley (1948). None of the early measurements gave any hint of their angular sizes which could well have been comparable with those of stars. However, some measurements of the positions of three of the stronger sources, Taurus-A, Virgo-A, and Centaurus-A, carried out by Bolton, Stanley, and Slee (1949) led them to suggest identifications of these sources with nebulae of unusual types. Later Mills and Thomas (1951) obtained a position for Cygnus-A which was very close to that of another faint nebula, although at that time no abnormality in the nebula was suspected.

The existence of localized sources of radiation with angular extents of the order of a degree was then demonstrated by Mills (1952*a*) and Piddington and Minnett (1952), some of whose preliminary results were described by Bracewell (1952). Although only one of these sources, Centaurus-A, could definitely be associated with a nebula, the large angular sizes of the others indicated a similar origin.

Further accurate position measurements (Smith 1951 ; Mills 1952*b*) appeared to confirm the identifications of the Taurus, Virgo, and Centaurus sources suggested earlier, and the position of the Cygnus source was found to be practically coincident with that of the faint nebula. Baade and Minkowski (1953*a*) found that this nebula consisted of two galaxies in collision and that the interstellar gas had a very high degree of excitation. They also found a peculiar and very faint galactic nebula in the position obtained by Smith for the Cassiopeia source.

At this stage it was clear that final evidence for the identifications would be agreement between the dimensions of the radio sources and the nebulae. Simultaneous attempts were made in Australia and England to construct

* Division of Radiophysics, C.S.I.R.O., University Grounds, Sydney.

equipment with the necessary resolving power, of the order of 1' of arc, to measure the radio sizes. Because of the high resolving power required, pencil-beam aerials were impractical and consequently interferometric methods were employed. These attempts were successful at approximately the same time and preliminary results have now been described. In England the sources Cassiopeia and Cygnus-A were observed by Brown, Jennison, and das Gupta (1952) and Smith (1952*a*, 1952*b*), and in Australia the sources Cygnus-A, Taurus-A, Virgo-A, and Centaurus-A,* by Mills (1952*c*). All five sources were resolved and found to have angular sizes comparable with their associated nebulae, thus verifying the identifications, but the measurements gave insufficient information from which to deduce the shapes and brightness temperatures of the sources.

The present paper gives the results of much more extensive observations carried out on the same four sources. They have led to more detailed knowledge. The equipment and techniques employed are also described more fully than in the preliminary note. It is found that there are certain similarities between the radio and optical features of the nebulae.

II. THEORY

The fundamental method of obtaining the brightness distribution across a source of radiation by means of interferometer observations was pointed out by McCready, Pawsey, and Payne-Scott (1947). By taking a number of observations with different aerial spacings along a common axis, it is possible to derive the "integrated" brightness distribution over the source, where the integrated brightness is the integral of the emission along a line at right angles to the projection of the interferometer axis on the source. If the radio isophotes are known to be circularly symmetric, this series of observations is sufficient to determine the actual surface brightness distribution. If the isophotes are central ellipses, it will be shown later that three sets of observations with three different interferometer axes will determine the actual brightness distribution. For more complex shapes even more sets of observations are necessary. In this work three sets of measurements have been made, extensive measurements with an interferometer axis at one azimuth angle (east-west) and one or two measurements at different azimuths. While there is no certainty that a true "radio picture" of a source can be constructed in this way, it is probable that valuable information can be obtained by comparing the radio and optical pictures. If very much more detailed information is required, pencil-beam methods are likely to lead to solutions more efficiently.

The relation between the aerial spacing, the distribution across the source, and the amplitude and phase of the interference pattern is derived in Appendix I. It is given by

$$I(\theta) = \int_0^{\infty} A_n \cos(\varphi_n + 2\pi n \theta) dn, \dots\dots\dots (1)$$

* These sources were designated 19+4, 05+2, 12+1, and 13-4 respectively by Mills (1952*a*, 1952*b*).

where $I(\theta)$ is the "integrated" brightness distribution across the source, a function of angle θ , n is the effective aerial spacing measured in wavelengths (see below), and A_n and φ_n are the relative amplitude and phase angle of the interference pattern.

The effective aerial spacing n is the projection on the wave front of the actual aerial spacing. It is related to the actual aerial separation, n' , the azimuth of the interferometer axis, A , and the zenith angle of the source, Z , by

$$n = n'(1 - \cos^2 A \sin^2 Z)^{\frac{1}{2}}. \dots\dots\dots (2)$$

For a source in which a sharp concentration is superimposed unsymmetrically on a larger diffuse area, the interference pattern will be the vector sum of two components due to the sharp concentration and diffuse area respectively. From the Fourier transform equation (1) it will be seen that the amplitude of the diffuse area component will fall off rapidly as the aerial spacing is increased; the sharp concentration component will not be reduced in the same proportion. The phase difference between these two components also depends on the aerial spacing, as well as the relative positions of the two sections of the source. Adding these components together, the resulting interference pattern will have an amplitude and phase which depend on the aerial spacing. At large spacings the diffuse area component will be negligible and the apparent position of the source will be that of the sharp concentration.

Determination of the phase angle φ_n implies the measurement of apparent position at each spacing. This could be done only with great difficulty with the present interferometer, so each source is assumed to be symmetrical. This allows φ_n to be put equal to zero in equation (1) and reduces it to a Fourier cosine transform. The assumption of symmetry is not unreasonable in view of the approximate symmetry of the nebulae associated with the radio sources. The same assumption has been made by Stanier (1950) and Machin (1951) in their work on the distribution of brightness across the Sun. One effect is to concentrate unsymmetrical features of the distribution into the central regions so that if the distribution is complex it is very likely that the brightness of the centre will be increased at the expense of the outer regions.

The surface brightness isophotes of a source may be investigated from the integrated brightness distributions along various axes. If the isophotes are concentric ellipses, then three axes are needed. In the general case for such ellipses the shape as well as scale varies along different axes, and a rather complicated normalizing procedure is required. In this work, however, it is found that the observations are consistent with distributions with the same shape but different scales along different axes. So the isophotes are assumed to have the same ellipticity and orientation.

The procedure for such a model is as follows. Firstly, for each axis the corresponding integrated distribution is used to determine the radial brightness distribution $B(r)$ for a circularly symmetrical model. It can easily be shown that $B(r)$ is the solution of the Abelian equation

$$I(\theta) = 2 \int_{\theta}^{\infty} \frac{B(r)r}{\sqrt{r^2 - \theta^2}} dr. \dots\dots\dots (3)$$

For each axis for the elliptical model it can be seen that the value of $B(r)$, determined by equation (3) for any value of θ , is now the brightness of the isophote which is tangential to the line $\theta = \text{constant}$. From the distributions of $B(r)$ corresponding to three different axes the complete isophotes may be constructed, the centre and three tangents to each elliptical isophote being known. This procedure is followed through in detail for a particular set of observations in Section V (a).

Machin (1951) has shown that $B(r)$ may be obtained directly from the relative amplitude curve by means of a Bessel transform. Here, however, the quantity $I(\theta)$ has been calculated first as it involves less assumptions and is therefore more fundamental; also it may be obtained with much greater accuracy. $B(r)$ has then been calculated from equation (3). An approximate solution to this equation has been developed which can be obtained very rapidly with an accuracy appropriate to the many assumptions involved.

The projection of the interferometer base across the source at transit will make some angle A' with the meridian. This angle is given by

$$\tan A' = \tan A / \cos Z, \dots\dots\dots (4)$$

where A is the interferometer azimuth and Z the zenith angle of the source.

The preceding analysis gives only the relative values of the surface brightness. Absolute values are required, however, and it is usual to quote the equivalent brightness temperature. At radio frequencies the Planck formula for thermal radiation reduces to the Rayleigh-Jeans form which, for constant frequency increments, is

$$T_0 = \frac{S\lambda^2}{2kfb\Delta\Omega}, \dots\dots\dots (5)$$

where T_0 is the central temperature, S is the flux density due to the source, k is Boltzmann's constant, λ is the wavelength, b is the normalized value of the surface brightness, and $d\Omega$ is an element of solid angle in steradians.

III. EQUIPMENT

Basically the equipment consists of a two-aerial interferometer, comprising a large fixed aerial and a small portable aerial, in which the radio-frequency connection between the portable aerial and the receiver is obtained by a radio link. By this means great flexibility is achieved in the possible placing of this aerial and spacings up to 10 km or more may be used.

The operating frequency of the interferometer is 101 Mc/s. It was chosen primarily because equipment of this frequency was available and it results in a convenient size for the portable aerial. A photograph of this aerial, which consists of two Yagis connected in parallel, is shown in Plate 1. The transmitting aerials for the radio link are also shown at the top of the vertical pole. The battery-operated receiving and transmitting equipment is in the trailer. The fixed 101 Mc/s receiving aerial is a broadside array with an area of 50 m². It has been described elsewhere (Mills 1952a).

A simplified block diagram of the complete equipment from which the operation can be followed is shown in Figure 1. Between it and the simpler types of interferometers described previously there are several differences which require detailed discussion. First is the radio link itself. Both the 101 Mc/s signal from the radio source, which is converted in frequency before transmission in order to avoid interaction effects, and the local oscillator frequency are transmitted at a level of about $\frac{1}{2}$ W. When these two signals are mixed at the receiving end of the link, the original 101 Mc/s signal is reconstructed with its phase changed by a constant amount. It is then available for mixing with the signal from the fixed aerial to form the interference pattern, although it is not practicable to do so immediately for several reasons.

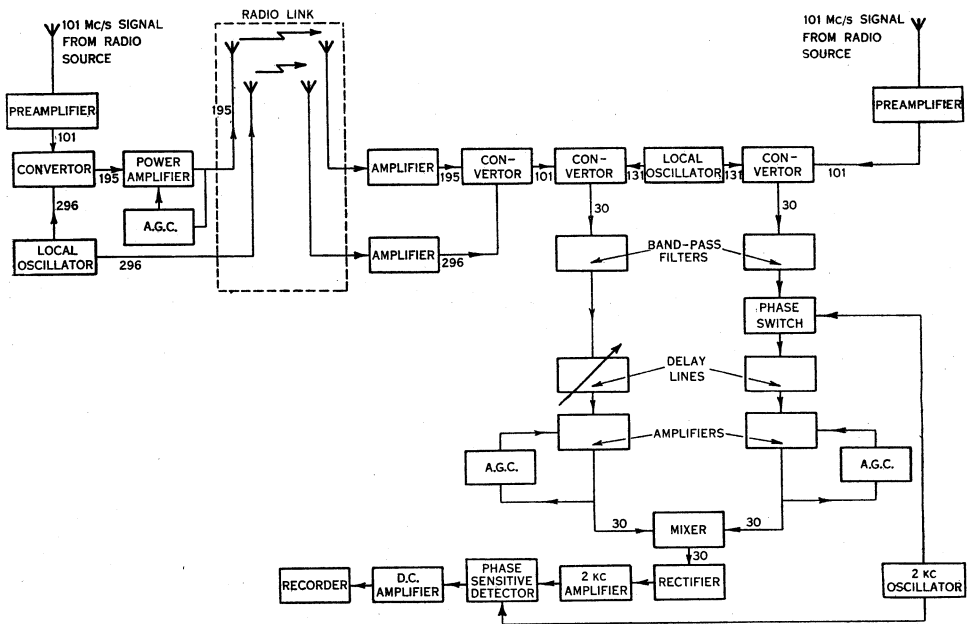


Fig. 1.—Block diagram of the complete equipment. Operating frequencies (in Mc/s) are indicated.

First, it is necessary to control the propagation times of the signals from each 101 Mc/s aerial to the mixing point. When these are equal and the radio source is in a plane at right angles to the interferometer axis, all the component frequencies within the pass band of the equipment arrive at the mixing point in the same phase and the interference pattern will have its maximum amplitude. When the propagation times are unequal, the phases of the component frequencies will be unequal and the pattern will be reduced in amplitude. The effect becomes more pronounced at large aerial spacings, and with a spacing of 10 km it confines the response of the interferometer to an angle of about $1\frac{1}{2}^\circ$ on either side of the central collimation plane. The collimation plane may be moved by changing the propagation time between one aerial and the mixing point. An analysis

of the effect in the case of a sea interferometer has been given by Stanley and Slee (1950). When the interferometer axis is east-west, the propagation times must be adjusted for equality at each different aerial spacing. When the aerial axis is not in an east-west direction, adjustment is required for different declinations in addition, since the collimation plane must be adjusted to intersect the meridian at the zenith angle of the source under observation. The most convenient means of obtaining the required variation is by the use of mercury-filled acoustic delay lines. It is difficult to construct a mercury line for very

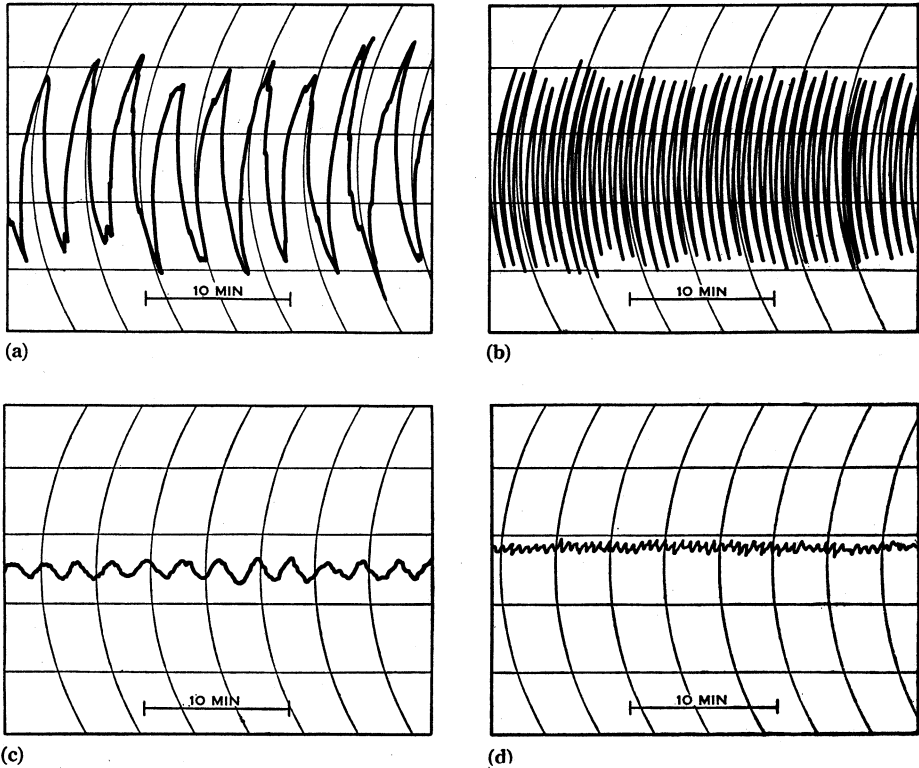


Fig. 2.—Some sample records.

- (a) Cygnus-A. Aerial spacing=0.29 km, E.-W., 29.ix.52.
- (b) Cygnus-A. Aerial spacing=1.25 km, E.-W., 29.iii.53.
- (c) Virgo-A. Aerial spacing=0.29 km, E.-W., 29.ix.52.
- (d) Virgo-A. Aerial spacing=1.25 km, E.-W., 3.iv.53.

short delays so that it is necessary to insert a delay in both signal paths. One is fixed at 60 μ sec and one variable from 60 to about 40 μ sec. Both signals are converted from 101 to 30 Mc/s by means of a common local oscillator before passing through the lines. This is necessary as the attenuation is excessive at the higher frequency.

A difficulty with the use of a radio link is that the amplitude stability is not particularly high. Since the amplitude of the interference pattern is a function of the individual amplitudes of each signal, it is necessary to stabilize them

before mixing. This is achieved by defining the pass band of each signal by two identical 30 Mc/s filters of approximately $\frac{1}{2}$ Mc/s bandwidth and then amplifying each signal to controlled equal levels of about 1 V. This ensures that the noise powers generated in each aerial and preamplifier system are equalized, so that, if the aerial gains and the noise factors do not vary and there is no other source of noise in the system, the overall sensitivity of the equipment will be constant. After mixing, the combined signal is rectified immediately without further amplification.

A phase switching system is also employed, operating at a frequency of 2 kc/s. While not essential for the operation of the equipment, it is convenient because it is difficult to obtain a very high degree of stability from the automatic gain controls. A high switching frequency is desirable because the period of the interference pattern is very short with the longer spacings.

Some sample records obtained with the equipment on different sources and at different spacings are shown in Figure 2.

IV. ACCURACY

There are many factors which can affect the accuracy of the relative amplitude measurements. For convenience, the sources of error are considered under five headings:

- (a) Time variations of sensitivity.
- (b) Characteristics of the portable aerial sites.
- (c) Confusion with other sources.
- (d) Reading errors in the presence of random fluctuations.
- (e) Systematic changes in sensitivity with distance.

The effect of the first four sources of error is to cause a more or less random dispersion of the measured amplitudes about their true values. Examination of the results of Section V show that there are no obvious effects of this kind. It is estimated that their total effect results in a probable error in the relative amplitudes of the Cygnus source of less than 5 per cent. at the closer spacings and less than 10 per cent. at the 5 and 10 km spacings. With the other sources the probable errors are thought to be less than 10 per cent.

The fifth source of error is particularly important because any systematic reduction in sensitivity as the aerial spacing is increased could result in an erroneous claim that a source had been resolved. It is thought that errors of this type are negligible.

(a) *Time Variations of Sensitivity*

Here are included all those parameters of the system which can affect the overall sensitivity at a fixed aerial spacing and which tend to vary with the passage of time. They include aerial gain, preamplifier sensitivity, signal-to-noise ratio on the radio link receivers, frequency pass bands, automatic gain control levels, and the sensitivity of the recorder and its amplifying system. The effect of such variables on the sensitivity was checked at intervals by returning the portable aerial to a fixed site and observing the amplitude of the pattern recorded on the Cygnus source. In the absence of actual equipment faults, the maximum range in sensitivity was about 15 per cent., and usually

the deflexion was within 5 per cent. of the mean value taken as standard. A device was also developed which could be used for testing the overall sensitivity, excluding the aerial gain, without moving the portable equipment. It consists of a diode noise generator which is connected to the input of a preamplifier and pulsed at the switching frequency of 2 kc/s. The switch frequency is then adjusted until there is a difference of about $\frac{1}{2}$ c/s. The result is a beat pattern on the recorder at the difference frequency, the amplitude of which gives a measure of the sensitivity of the equipment.

(b) Characteristics of the Portable Aerial Sites

Variations in sensitivity at different sites can occur due to differences in the ground reflection effects and to differences in the propagation conditions over the radio link. Errors due to ground reflections were reduced to a minimum by selecting the various sites to be as flat and as free from obstructions as possible, and where necessary calculating corrections due to the ground reflected wave.

Providing the signal-to-noise ratio at the receiving end of the link is high it can have no effect on sensitivity. This was usually the case, but in one or two instances, particularly with the maximum spacing of 10 km where the signal-to-noise ratio was as low as 10 db, a correction had to be applied.

(c) Confusion with Other Sources

In addition to the source under observation, the aerials receive radiation from a large number of weaker sources. These will affect the relative amplitudes at each spacing in a random way. Errors of this type have been discussed by Smith (1952*b*), but his suggestion that a large number of observations will enable the error to be eliminated appears to be wrong, for there seems to be no way in which the component due to the wanted source may be separated, unless phases are measured.

(d) Reading Errors in the Presence of Random Fluctuations

A limit to the reading accuracy is set by the random noise fluctuations of the recorder, but they become important only when the relative amplitudes are low. Signal-to-fluctuation level at 1 km spacing ranges from about 5 for the Centaurus source to about 60 for the Cygnus source. A large number of recorder oscillations are averaged in every case to reduce this error to a minimum.

(e) Systematic Changes in Sensitivity with Distance

There are several factors which could lead to a reduction in sensitivity as the aerial spacing is increased. Because of their fundamental nature, errors of this type have received special attention and it is considered that the equipment is completely free from them, at least to a spacing of 5 km, and probably to many times this distance. Two possible sources of this kind of error in the equipment are phase instability, in which the variations in phase are more rapid than the recording system can follow, and frequency dispersion. Phase instability due to propagation changes and frequency dispersion both cause errors which tend to become worse as the length of the radio link is increased.

Possible phase instability was checked using 101 Mc/s transmissions from a small transmitter, which were received by both aerials and compared in phase

at the mixing point. This test was carried out with spacings of 1 and 5 km. It was found that in each case there were slow drifts in phase of up to 60° in an operating period of about $\frac{1}{2}$ hr, but that rapid drifts which could probably not be followed by the recorder in normal operation had an r.m.s. value of less than 3° . Because the results were similar on both spacings it is thought that the effects originated in the equipment rather than in the radio link. In any case they were so small as to have a negligible effect on the amplitude of the interference pattern.

The effect of dispersion was not expected to be important both because of theoretical considerations and because of practical experience with pulsed transmission systems. It was tested at the 5 km spacing by replacing the $\frac{1}{2}$ Mc/s filters defining the pass band of the equipment by filters with a bandwidth of about 140 kc/s. If dispersion were present and the total output power from the receiver were kept constant, the amplitude of the interference pattern due to a source would be increased with the narrower bandwidth. There was no significant difference in the amplitudes so that the effect of dispersion can be ignored.

A further possible source of error of this type could be due to the presence of ionospheric irregularities. As far as the effects of the irregularities are understood at present, however, it does not appear likely that they could produce any systematic effect. This was confirmed when observations were being made on the Cygnus source with spacings of both 5 and 10 km, when some records were steady in both phase and amplitude while others showed the same sorts of fluctuations as are commonly observed with closer spacings. Only the steady records were used to obtain the relative amplitudes of the source.

Finally, at the longer spacings the period of the interference pattern becomes so short (approximately 5 sec at 10 km) that allowance must be made for a reduction in the response of the recording system. This was overcome to a certain extent by using a shorter integrating time constant at these spacings. Values used were 2 sec out to 1.5 km and $\frac{1}{2}$ sec for the 5 and 10 km observations. The necessary small corrections were then calculated.

V. MEASUREMENTS AND ANALYSIS

Observations were made on the sources Taurus-A, Virgo-A, Centaurus-A, and Cygnus-A with nine different spacings in an east-west direction ranging from 60 m to 10 km and with three spacings at other azimuths. The east-west observations were sufficiently numerous to obtain distributions in that direction with an accuracy appropriate to the assumption of symmetry. Of the other observations one set has been made at an azimuth of 164° (east of north) and a spacing of approximately 1 km and the other two at an azimuth of 24° and spacings of 1 and 2 km. These are adequate to orient the major and minor axes of the sources approximately without giving very much information about their distributions in these directions. A few more observations would have been desirable, but the necessity of concluding the investigation within a definite time limit prevented any further observational work. The measurements on each source and their analysis will now be considered in turn.

(a) *Taurus-A*

The observations on this source are given in Table 1 ; also given is a measurement made with a different interferometer (Mills 1952*b*) at a close spacing of 60 m which sets an upper limit to the value of the relative amplitude at this spacing.

TABLE 1
OBSERVATIONS OF THE RELATIVE AMPLITUDE OF TAURUS-A WITH DIFFERENT AERIAL SPACINGS AND AZIMUTHS

Azimuth of Interferometer Axis	Aerial Spacing (km)	n (wavelengths)	Relative Amplitude
90°	0.06*	20	<1.06
	0.29	100	1.00
	0.50	168	0.79
	0.79	265	0.77
	1.02	344	0.55
	1.25	420	0.47
	1.54	518	0.35
	5.35	1800	†
10.01	3400	†	
164°	0.94	192	0.72
24°	1.01	219	0.87
	2.10	455	0.53

* Observations made with different equipment.

† The amplitude of the interference pattern was less than the noise fluctuations of the equipment. The relative amplitude is less than about 0.1.

These values are plotted in Figure 3 (a) and a smooth curve drawn through the east-west points to give the *amplitude-aerial spacing spectrum*. Inspection of the points obtained in the other directions shows that the source is not circularly symmetric as its apparent extent is less when measured at the 24° azimuth (since the amplitude falls off less rapidly).

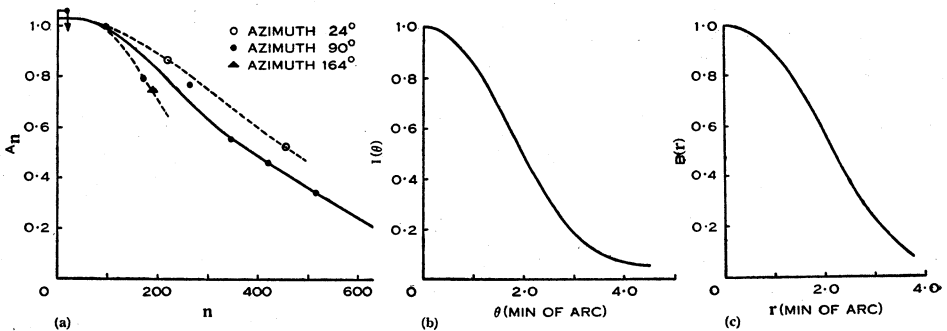


Fig. 3.—Taurus-A.

- (a) Amplitude-spacing spectra.
- (b) Integrated brightness distribution, E.-W.
- (c) Maximum surface brightness distribution, E.-W.

In Figure 3 (b) is shown the integrated brightness distribution obtained from equation (1) by putting φ_n equal to zero. The effective size defined before (Mills 1952c) as the angle between the half-brightness points on this curve is $4.0'$. In Figure 3 (c) is shown the equivalent radial brightness distribution derived from equation (3). There is little difference between this and the integrated brightness distribution.

The shape and orientation of the isophotes may be estimated from the measurements made in the other directions. There is insufficient information to construct the brightness distributions in these directions with any accuracy, so the assumption is made that the shapes of the distributions are the same in all directions. This places the further restriction on the isophotes that they should have the same ellipticity; it is consistent with the two observations at an azimuth of 24° . The isophotes may now be constructed. From equations

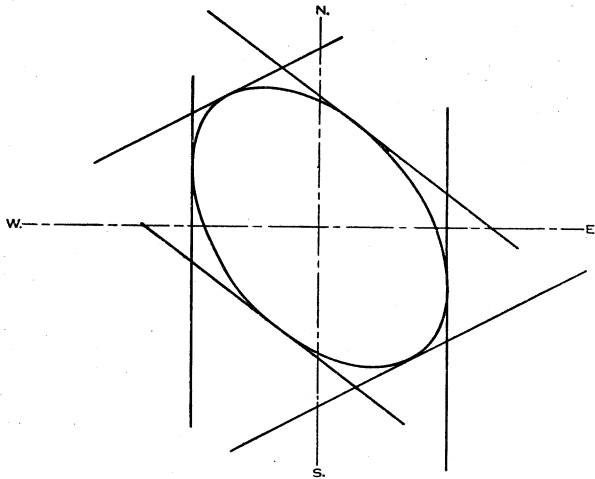


Fig. 4.—Construction of the half-brightness isophote of Taurus-A.

(1) and (3) and the description of method already given it will be seen that the relative separation of the extremities of an isophote in any direction is inversely proportional to the abscissae of the intersections of the appropriate amplitude spectrum curve with any convenient ordinate. An ordinate of $A_n=0.7$ has been chosen, giving intercepts at $n=265$ for the east-west distribution, $n=210$ for an azimuth of 164° , and $n=330$ for an azimuth of 24° .

Taking the half-brightness isophote as the most suitable one to construct as it is least sensitive to variations in the amplitude spectrum, the separations of the extremities of the isophote in these directions become $4.3'$, $5.4'$, and $3.5'$ respectively. The position angles corresponding to the above azimuth angles are then calculated from equation (4), and in Figure 4 the extensions are drawn at right angles to the position angles and the elliptical isophote drawn tangentially to these enclosing lines. The isophote has a size of $5\frac{1}{2}$ by $3\frac{1}{2}'$ with the major axis in position angle 140° .

The average central equivalent temperature of the source may now be estimated. On the basis of the dimensions above and the brightness distribution of Figure 3 (c), and by applying equation (5), this temperature is found to be 4×10^6 °K. Actual temperatures could exceed this by large amounts because a fine structure could exist and not be revealed by the present observations.

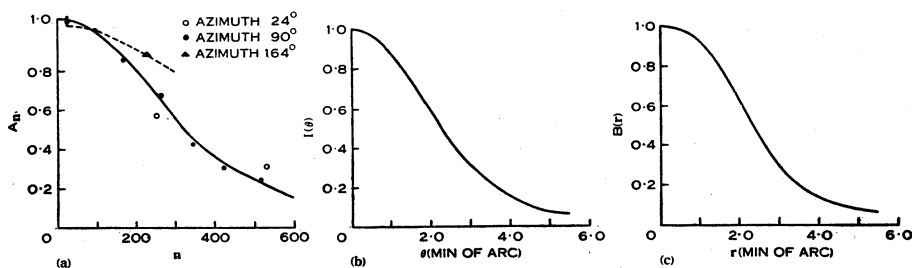


Fig. 5.—Virgo-A.

- (a) Amplitude-spacing spectra.
 (b) Integrated brightness distribution, E.-W.
 (c) Maximum surface brightness distribution, E.-W.

(b) *Virgo-A*

The Virgo source has been treated similarly. The observational results are collected in Table 2 and the amplitude spectrum and the integrated and surface brightness distributions are plotted in Figures 5 (a)–(c). The east-west effective size is 4.6'.

TABLE 2
 OBSERVATIONS OF THE RELATIVE AMPLITUDE OF VIRGO-A WITH DIFFERENT AERIAL SPACINGS AND AZIMUTHS

Azimuth of Interferometer Axis	Aerial Spacing (km)	n (wavelengths)	Relative Amplitude
90°	0.06*	20	<1.06
	0.29	100	1.00
	0.50	168	0.85
	0.79	265	0.67
	1.02	344	0.42
	1.25	420	0.30
	1.54	518	0.24
	5.35	1800	†
	10.01	3400	†
164°	0.94	226	0.88
24°	1.01	252	0.57
	2.10	525	0.31

* Observation made with different equipment.

† The amplitude of the interference pattern was less than the noise fluctuations of the equipment. The relative amplitude is less than about 0.1.

In obtaining the dimensions and orientation of the half-brightness contour there is a little difficulty, as it appears from the amplitude spectrum that the

distribution with the 24° azimuth is slightly different from the east-west distribution, showing a sharper concentration towards the centre and wider skirts. However, the difference barely exceeds the accuracy of the observations so that the distributions have been assumed to be identical and the half-brightness ellipse drawn as before. The size is then 5 by $2\frac{1}{2}'$ with the major axis in position angle 50° .

An estimate of the average central equivalent temperature gives 4×10^6 °K. Again the presence of fine detail could result in much higher temperatures.

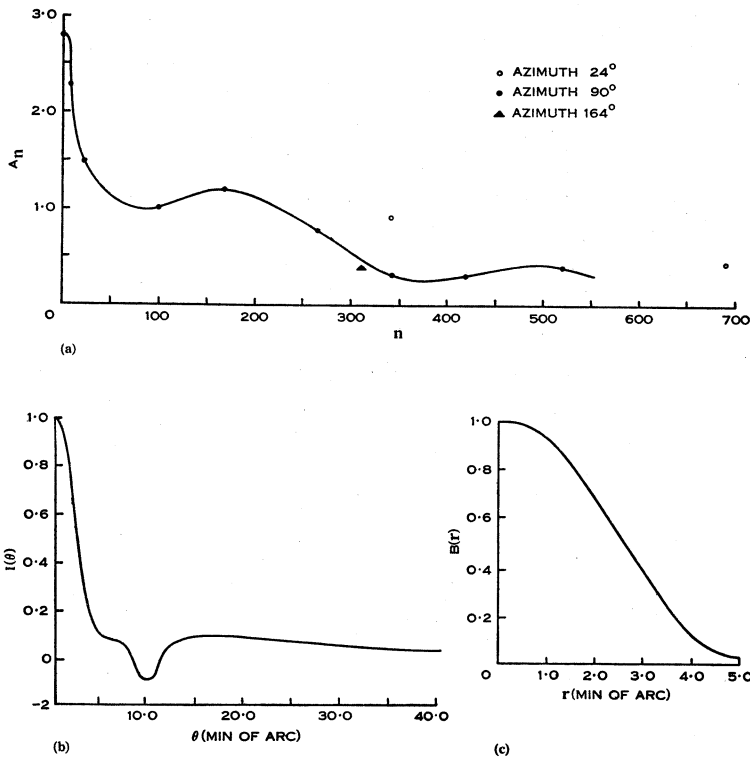


Fig. 6.—Centaurus-A.

- (a) Amplitude-spacing spectra.
 (b) Integrated brightness distribution, E.-W.
 (c) Maximum surface brightness distribution, E.-W.

(c) *Centaurus-A*

This source presents special difficulties, as it has already been shown that it has a complicated distribution consisting essentially of an extended source of large angular size with a strong concentration near, but not coincident with its centre.* It is now found in addition that the amplitude spectrum of the complex object has puzzling features.

In order to construct the east-west spectrum as accurately as possible, the present observations were supplemented by the results of two observations

* Reported by J. G. Bolton at U.R.S.I. General Assembly 1952.

with different equipments, (i) interferometer observations with a spacing of 60 m and (ii) an observation of the total intensity of the source obtained with the pencil-beam aerial described by Mills and Little (1953). The results of the observations are given in Table 3, and the amplitude spectra and the integrated and surface brightness distributions in Figures 6 (a)–(c).

An inspection of Figure 6 (b) reveals that over a small angle the derived integrated brightness is negative, which is a physical impossibility. The amplitude spectrum of Figure 6 (a) would therefore appear to be incorrect. A possibility that suggests itself is that the amplitudes at $n=420$ and $n=518$ could be negative, since no check is kept on their phases. A smooth curve could then be drawn through the points again, but this would lead to negative excursions

TABLE 3
OBSERVATIONS OF THE RELATIVE AMPLITUDE OF CENTAURUS-A WITH DIFFERENT
AERIAL SPACINGS AND AZIMUTHS

Azimuth of Interferometer Axis	Aerial Spacing (km)	n (wavelengths)	Relative Amplitude
90°	0*	0	2.80
	0.021	7	2.30
	0.060*	20	1.50
	0.29	100	1.00
	0.50	168	1.20
	0.79	265	0.80
	1.02	344	0.33
	1.25	420	0.33
	1.54	518	0.40
	5.35	1800	†
	10.01	3400	†
164°	0.94	313	0.40
24°	1.01	337	0.92
	2.10	700	0.40

* Observation made with different equipment.

† The amplitude of the interference pattern was less than the noise fluctuations of the equipment. The relative amplitude is less than about 0.2.

of brightness of much larger amplitude and is therefore unlikely to be correct. Some such anomaly is not surprising, however, as symmetry has been assumed and it may not exist. The result is salutary in demonstrating the errors which may arise owing to such an assumption. Another reason may be the omission of components due to spacings between 1.5 and 5 km, which could be appreciable. Because of the above anomaly the radial brightness distribution curve has been drawn only over the central concentration.

Two comparatively reliable results which can be obtained from the curves are that approximately 45 per cent. of the total energy of the source is in the central concentration and it has an effective size east-west of 5'. The effective size of the extended portion is difficult to estimate but it is of the order of $1\frac{1}{2}^\circ$.

An attempt has also been made to construct the half-brightness isophote of the central concentration and estimate the central temperature as before. The same assumption of spectra of similar shapes in every direction is made which is consistent with the observed points. The size of the ellipse is then $6\frac{1}{2}$ by $3'$ with the major axis in position angle 130° . While the accuracy is not expected to be very good, it seems quite clear that the extension of the source measured with an azimuth of 24° is much less than in the other directions.

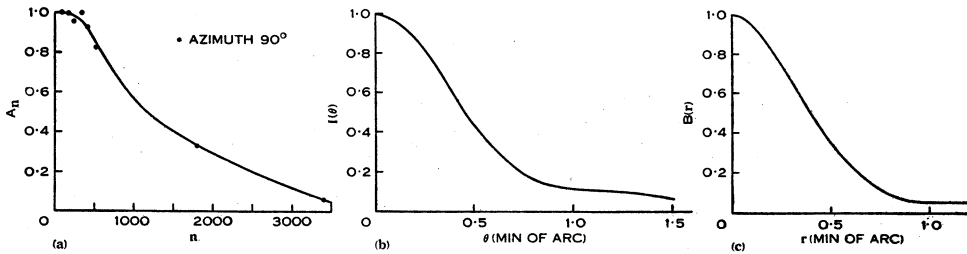


Fig. 7.—Cygnus-A.

- (a) Amplitude-spacing spectrum.
- (b) Integrated brightness distribution, E.-W.
- (c) Maximum surface brightness distribution, E.-W.

Estimates of the equivalent temperatures give 4×10^6 °K for that of the central concentration and a value of the order of 3×10^4 °K for the brightest portions of the extended source (on the assumption of circular symmetry in the latter case).

(d) *Cygnus-A*

The observations on this source are tabulated in Table 4. Only the east-west observations are given as no significant changes in amplitude were detected in the other directions. This is not surprising as, with the large zenith angle of the source at Sydney, the effective aerial separations in these directions as given by equation (2) are very small.

TABLE 4
OBSERVATIONS OF THE RELATIVE AMPLITUDE OF CYGNUS-A WITH DIFFERENT SPACINGS IN AN EAST-WEST DIRECTION

Aerial Spacing (km)	n (wavelengths)	Relative Amplitude
0.29	100	1.00
0.50	168	1.00
0.79	265	0.98
1.02	344	1.00
1.25	420	0.93
1.54	518	0.83
5.35	1800	0.33
10.01	3400	0.06

In Figure 7 (*a*) these points are plotted and a smooth curve is drawn through them. There are insufficient observations at large spacings to define this curve with certainty, and indeed it could well cross the zero axis several times. However, as drawn, it possesses the same features of a comparatively rapid initial fall and a long "tail" which is characteristic of the spectra of the other sources and in addition it is physically plausible.

The integrated brightness distribution $I(\theta)$ and the surface brightness distribution $B(r)$ are shown in Figures 7 (*b*) and 7 (*c*) respectively. From the latter curve can be calculated an average central equivalent temperature of the source on the assumption of circular symmetry. It is equal to 6×10^8 °K. Since the observations of Brown, Jennison, and das Gupta (1952) have shown that the Cygnus source is decidedly elongated with its longer axis not far from the east-west direction, the actual temperature is likely to be several times this value. Also it should be pointed out that the observations have been taken only to a distance of 10 km, so that the possibility of finer detail in the brightness distribution should not be overlooked.

VI. DISCUSSION

In Section V a certain amount of information about the properties of the sources was extracted from the observations. It now remains to consider these properties in relation to the nebulae with which the sources are identified and to try to draw some general conclusions. Various properties of the sources and related nebulae are tabulated in Table 5. A large part of the information concerning the nebulae is due to Baade and Minkowski (1953*a*, 1953*b*).

A further comparison between the Taurus, Virgo, and Centaurus sources and their respective nebulae is shown in Plate 2, where photographs of the nebulae are compared directly with "radio pictures" of the sources constructed from the data derived in Section V. While there is no particular reason why the radio isophotes should agree with optical features of the nebulae, it is clear that there are marked similarities, especially for two of the sources. The sources will now be discussed in turn.

First consider the Cygnus source and its associated nebula. Baade and Minkowski describe the nebula as having a bright central region of about 3 by 5" surrounded by a much larger fainter part of elliptical outline, about 18 by 30" with the major axis in position angle 150°. From Figure 7 it is seen that the radio source has an effective size in an east-west direction of about 45". This is larger than the nebula but of the same order of size. Baade and Minkowski have shown that the nebula consists of two galaxies in collision, so presumably it is the excited interstellar gas which is responsible for the radio-frequency radiation, and it is not surprising that the gas should extend beyond the visible nucleus. Since it is unlikely that the temperature of the gas could rise as high as 6×10^8 °K or more as the result of a collision, it is probable that a non-thermal origin must be invoked for the radiation. This is also indicated by the spectrum of the source (Stanley and Slee 1950) which could not be produced by thermal emission from a hot, optically thin gas.

The Taurus source can be compared with its associated nebula, the Crab nebula, in rather more detail, as there is more information concerning the radio source and the nebula has been the subject of extensive investigations. Here the optical and radio shapes are very similar. It is well known that the nebula consists of an amorphous mass of gas at a temperature which has been estimated as 50,000 °K (Minkowski 1942), together with a filamentary network. From the radio observations it is impossible to decide which of these features is responsible for the radiation, although it appears likely that it originates over

TABLE 5
A COMPARISON BETWEEN THE RADIO SOURCES AND THEIR ASSOCIATED NEBULAE

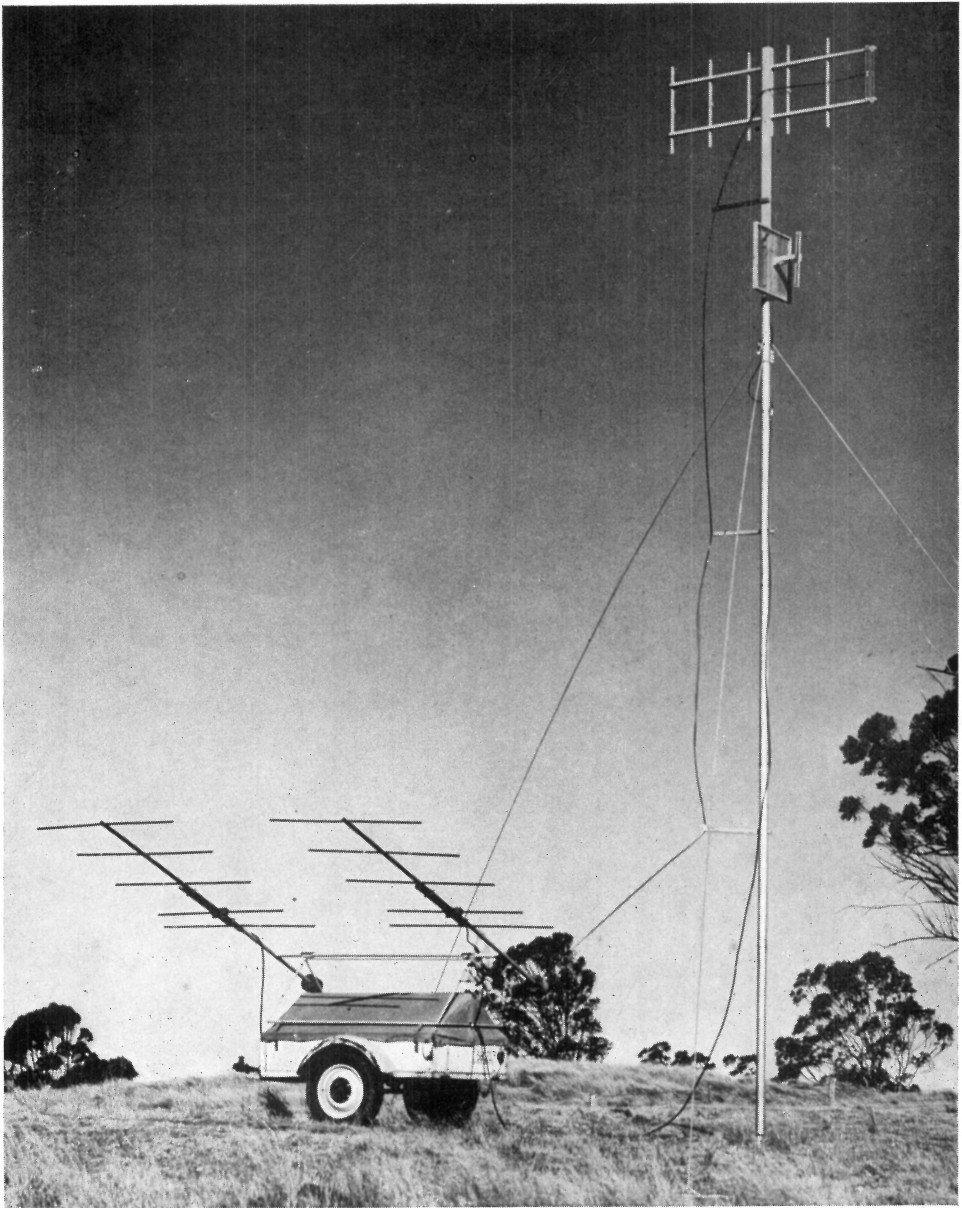
Radio source		Taurus-A	Virgo-A	Centaurus-A	Cygnus-A
Nebula		NGC 1952	NGC 4486	NGC 5128	—
Nebula type		Galactic, Supernova remnant	Extra-galactic, E ₀	Extra-galactic, Peculiar	Extra-galactic, Two galaxies in collision
Magnitude	Radio m_R^*	3.4	3.8	3.4	1.3
	Photographic m_p	9.0	9.9	7.2	17
Angular size	Radio source—effective size E.-W.	4.0'	4.6'	5.0'	45"
	Radio source ($\frac{1}{2}$ brightness)	5½ by 3½'	5 by 2½'	6½ by 3' (Central concentration)	45"
	Nebula (approx.)	6 by 4'	5 by 5'	6 by 6' (to $\frac{1}{2}$ brightness)	30 by 18"
Position angle	Radio source	140°	50°	130°	—
	Nebula	120°	—	—	150°
	Abnormal features of nebula	—	A "jet" at 290°	Obscuring band at 135°	—
Central equivalent brightness temperature of radio source		≈ 4 × 10 ⁶ °K	≈ 4 × 10 ⁶ °K	≈ 4 × 10 ⁶ °K	> 6 × 10 ⁸ °K

* The magnitude system of Brown and Hazard (1952) is used here, i.e. $m_R = -5.3 \cdot 4 - 2.5 \log_{10} S$, where S is the flux density in $W m^{-2} (c/s)^{-1}$.

the whole space occupied by the nebula. The central temperature of the source seems far too high to be explained in terms of thermal radiation from the mass of gas, although Stanley and Slee (1950) suggest that the spectrum is compatible with such an origin. However, the latest results of Stanley, Slee, and Bolton (personal communication) contradict the previous results and suggest a spectrum more like that of the other sources. It seems probable that a non-thermal process is operative in the gaseous mass of the nebula as also appears likely in the case of the Cygnus source.

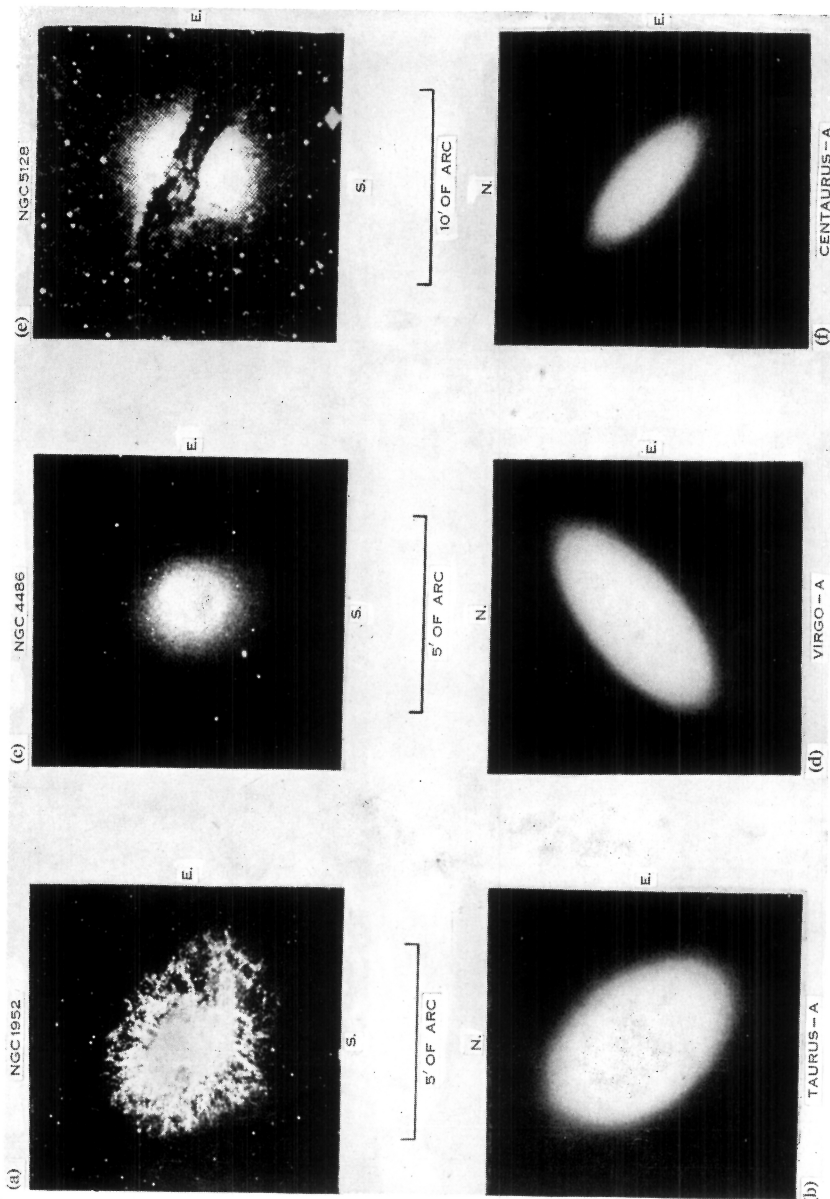
The nebula NGC 4486 which is associated with the source Virgo-A is very peculiar. It appears to be a typical E₀ galaxy which has the unique feature

RADIO BRIGHTNESS DISTRIBUTION OF COSMIC NOISE



The portable aerial and associated equipment. Subsequently the receiving Yagi aeriels were removed to a distance of about 10 m from the transmitting equipment to avoid troublesome interaction effects.

RADIO BRIGHTNESS DISTRIBUTION OF COSMIC NOISE



Photographs of the associated nebulae compared directly with "radio pictures" of the sources constructed from the observational data.

of a bright strip or "jet" of unknown composition crossing the nucleus at a position angle of about 290° . This jet is not visible in the photograph in Plate 2. Neither the nebula as a whole which is circular nor the jet which has a visible extent of only about $20''$ of arc and is nearly at right angles to the major axis of the radio source agrees precisely with the shape of the source. However, the length of the major axis of the source is of the same order as the overall diameter of the nebula so that it appears likely that the radio emission is associated with the nebula as a whole rather than with the jet, although, with the present observations, the possibility that the radiation is produced by an irregular line source contained within the region of the assumed elliptical isophotes cannot be excluded.

The central concentration of the Centaurus source appears to be definitely associated with the central portion of the galaxy NGC 5128, and in particular with the obscuring band which crosses the galaxy. Since we might expect to find a concentration of gas in this region it would appear that this source also, along with Cygnus, Taurus, and possibly the Virgo sources, could have its origin in interstellar gas; and again the temperature seems too high and the spectrum unlikely for a thermal origin. The extended source is rather more of a puzzle, but de Vaucouleurs (personal communication) has found that the nebula extends to a radius of at least $50'$ so that an association between the extended source and the outer regions of the nebula is not unlikely.

In conclusion it might be pointed out that the surface brightness temperatures of three of the sources are similar, suggesting a possible origin in similar processes carried on at about the same level of intensity. The exceptionally high surface temperature of the Cygnus source is not surprising in view of the extreme effects which might be expected to occur in such a rare event as the head-on collision of two galaxies.

VII. ACKNOWLEDGMENTS

The author is indebted to Mr. A. W. L. Carter for the preparation of Plate 2 and for assistance in constructing the equipment, making observations, and preparing the manuscript, to Mr. H. Harant for designing and constructing portion of the equipment including the mercury delay lines, and to Mr. A. Watkinson for maintaining and servicing the equipment and making observations.

VIII. REFERENCES

- BAADE, W., and MINKOWSKI, R. (1953a).—Identification of the radio sources in Cassiopeia, Cygnus-A, and Puppis-A. *Astrophys. J.* (in press).
- BAADE, W., and MINKOWSKI, R. (1953b). On the identification of radio sources. *Astrophys. J.* (in press).
- BOLTON, J. G., and STANLEY, G. J. (1948).—*Nature* **161**: 312.
- BOLTON, J. G., STANLEY, G. J., and SLEE, O. B. (1949).—*Nature* **164**: 101.
- BRACEWELL, R. N. (1952).—*Observatory* **72** (866): 27.
- BROWN, R. H., and HAZARD, C. (1952).—*Phil. Mag.* **43**: 137-52.
- BROWN, R. H., JENNISON, R. C., and DAS GUPTA, M. K. (1952).—*Nature* **170**: 1061.
- MACHIN, K. E. (1951).—*Nature* **167**: 889.
- MC CREADY, L. L., PAWSEY, J. L., and PAYNE-SCOTT, RUBY (1947).—*Proc. Roy. Soc. A* **190**: 357-75.
- MILLS, B. Y. (1952a).—*Aust. J. Sci. Res. A* **5**: 266-87.

- MILLS, B. Y. (1952b).—*Aust. J. Sci. Res. A* 5: 456-63.
 MILLS, B. Y. (1952c).—*Nature* 170: 1063.
 MILLS, B. Y., and LITTLE, A. G. (1953).—*Aust. J. Phys.* 6: 272-8.
 MILLS, B. Y., and THOMAS, A. B. (1951).—*Aust. J. Sci. Res. A* 4: 158-71.
 MINKOWSKI, R. (1942).—*Astrophys. J.* 96: 199.
 PIDDINGTON, J. H., and MINNETT, H. C. (1952).—*Aust. J. Sci. Res. A* 5: 17-31.
 SMITH, F. G. (1951).—*Nature* 168: 555.
 SMITH, F. G. (1952a).—*Nature* 170: 1065.
 SMITH, F. G. (1952b).—*Proc. Phys. Soc. Lond. B* 65: 971-80.
 STANIER, H. M. (1950).—*Nature* 165: 354.
 STANLEY, G. J., and SLEE, O. B. (1950).—*Aust. J. Sci. Res. A* 3: 234-50.

APPENDIX I

Calculation of the "Integrated" Brightness Distribution

For a point source the normalized response of an interferometer in a direction near the collimation plane is given very closely by

$$R(n, \theta) = \cos(2\pi n \theta),$$

where n is the effective aerial spacing in wavelengths and θ is the angle between the source direction and collimation plane.

For a distributed source of "integrated" brightness $I(\theta)$, the response is obtained by applying R to I thus,

$$G(n, \xi) = \int I(\theta) R(n, \theta - \xi) d\theta.$$

The integration is carried out over the primary aerial beam, but, since the angle of this beam is very much greater than the angular width of $I(\theta)$, the integration limits may be made infinite without sensible error. We then have,

$$G(n, \xi) = \int_{-\infty}^{+\infty} I(\theta) \cos(2\pi n \theta - \xi) d\theta.$$

Introducing complex notation,

$$A_n \exp(-i\varphi_n) \exp(-i2\pi n \xi) = \int_{-\infty}^{+\infty} I(\theta) \exp(i2\pi n \theta - \xi) d\theta,$$

where A_n is the relative amplitude and φ_n the relative phase of the interferometer output.

Eliminating $\exp(-i2\pi n \xi)$ we have

$$A_n \exp(-i\varphi_n) = \int_{-\infty}^{+\infty} I(\theta) \exp(i2\pi n \theta) d\theta,$$

whence

$$\begin{aligned} I(\theta) &= \int_{-\infty}^{+\infty} A_n \exp(-i\varphi_n) \exp(-i2\pi n \theta) dn \\ &= 2 \int_0^{\infty} A_n \cos(\varphi_n + 2\pi n \theta) dn. \end{aligned}$$

Only relative values of $I(\theta)$ are used in the analysis, so that the factor 2 may be omitted.